Ionization of uracil in collisions with highly charged carbon and oxygen ions of energy 100 keV to 78 MeV

A. N. Agnihotri,[1] S. Kasthurirangan,[2] S. Nandi,[1] A. Kumar,[3] M. E. Galassi,[4] R. D. Rivarola,[4] O. Fojón,[4] C. Champion,[5] J. Hanssen,[5] H. Lekadir,[5] P. F. Weck,[6] and L. C. Tribedi[1,*]

[1]*Department of Nuclear and Atomic Physics, Tata Institute of Fundamental Research, Colaba, Mumbai 400005, India*

[2]*Department of Physics, Institute of Chemical Technology, Matunga, Mumbai 400019, India*

[3]*Nuclear Physics Division, Bhabha Atomic Research Centre, Trombay, Mumbai 400 085, India*

[4]*Laboratorio de Colisiones Atómicas, Instituto de Física Rosario, Universidad Nacional de Rosario and CONICET, Av. Pellegrini 250, 2000 Rosario, Argentina*

[5]*Laboratoire de Physique Moléculaire et des Collisions, Université Paul Verlaine-Metz, F-57012 Metz Cedex 01, France*

[6]*Department of Chemistry, University of Nevada, Las Vegas, Nevada 89154, USA*

(Received 30 August 2011; published 26 March 2012)

Fast highly charged C and O ion-induced total ionization of an RNA base molecule, uracil ($C_4H_4N_2O_2$, $m = 112$ amu), has been investigated in a wide energy range of keV to MeV. A combined study of the collision products using a time-of-flight mass spectrometer and an electron spectrometer allows one to determine absolute total ionization cross sections (TCSs). Experimental measurements of TCSs are compared to theoretical predictions performed in the classical trajectory Monte Carlo and classical over-barrier (CTMC-COB) and quantum mechanical (Continuum Distorted Wave with Eikonal Initial State and first-order Born with correct boundary condition) frameworks. The overall energy dependence of the TCSs is approximately reproduced by the models, especially well in the high energy range. The CTMC-COB model provides an excellent agreement for the high-energy data. The projectile charge-state q dependence of TCSs deviates from the well-known quadratic behavior in ion-atom collisions.

DOI: 10.1103/PhysRevA.85.032711 PACS number(s): 34.50.Gb, 82.30.Fi

I. INTRODUCTION

Ionization of atoms and molecules by fast charged particles has been a matter of active research in the past few decades and is nowadays a well-documented subject with numerous applications in diverse areas such as atmospheric physics, plasma physics, medical physics, and astrophysics. Particularly in recent years, atomic collisions involving large molecules, bio-molecules, clusters, fullerenes, polycyclic aromatic hydrocarbons, other nanoparticles, and mesoscopic objects have attracted a great deal of attention. Theoretical models as well as experimental data on ion-induced collisions particularly for heavy ions such as carbon ions whose relevance has been clearly highlighted versus protons for hadron therapy are crucial in modeling the cell-damage processes. In this context, ion-induced collisions on biologically relevant targets such as DNA and RNA components (bases, sugar, and phosphate backbone) are of great importance. In heavy-ion therapy, the energy loss of swift ions is continuous and nonuniform along the ion track. Ions lose maximum energy in the Bragg peak region. Therefore, the study of the interaction of energetic ions with nucleobases over a wide energy range is necessary to model the actual radiation damage. The projectile energy range studied here falls broadly within the Bragg peak region and therefore is crucial for model calculations. A comparison of the experimental investigations with the state-of-the-art theoretical models for uracil will help explain the collisional mechanisms involving other large molecules or clusters. Until now measurements on such biological systems have been scarce and essentially limited to studies of radiation damage only explored at the mesoscopic scale and not at the single-molecule scale. Whereas fragmentation modes induced by low-energy multiply charged ions on isolated nucleobases were studied extensively [1–6], similar investigations about the ion-induced ionization on such molecules were only rarely reported, except for a few [7–10].

II. THEORETICAL MODELS

On the theoretical side, ion collisions with the DNA base molecules have been less studied, except for electron-induced ionization studies [11,12]. We essentially find two approaches: the classical trajectory Monte Carlo (CTMC) method [13], which is now combined with the classical over-barrier (COB) criteria [14,15], and the quantum-mechanical approach, where the differential and total ionization cross sections within the first-order Born framework for DNA bases are addressed [16,17]. Here we focus on measurements of absolute total ionization cross sections and their comparisons with theoretical predictions using the CTMC-COB, the continuum distorted wave-eikonal initial state (CDW-EIS), and eikonal initial-state (EIS), and first-order Born with correct boundary condition (CB1) calculations. The models based on the CDW-EIS and the CB1 calculations for uracil are developed in this work. In order to represent the 29 orbitals of uracil in its fundamental state, calculations based on the restricted Hartree-Fock method with geometry optimization [17] are done. We have adopted this molecular description to avoid the extreme difficulty of implementing more sophisticated ones, such as those based in the density-functional theory [18], in the dynamic electron ionization reaction of complex molecules.

*lokesh@tifr.res.in

Orbital energies were obtained with the GAUSSIAN09 software at the RHF-21G level [19]. Furthermore, each molecular orbital is described by a linear combination of atomic wave functions corresponding to the uracil compounds. This description is here employed to provide a one-active-electron representation. Thus, all possible final residual target states are implicitly included. Within the CB1 approximation [17,20], differential and total cross sections are computed in the case of ionization of uracil. In addition, a one-active-electron CDW-EIS approximation is also introduced here. In the CDW-EIS approximation, each of the molecular orbitals described above is distorted by a continuum projectile eikonal continuum in the initial channel while in the exit channel the continuum state of the ionized electron in the field of the residual target is distorted by a projectile continuum factor [21,22]. In both the CB1 and CDW-EIS approximations, effective Coulomb wave functions are employed to represent the continuum of the electron in the field of the residual target, with an effective nuclear charge $\xi = \sqrt{-2n_{ji}^2\epsilon_j}$. Here ϵ_j is the energy of the jth orbital and n_{ji} is the principal quantum number of the corresponding ith atomic wave function composing this orbital one. Total cross sections within the CTMC-COB model are also computed, where only the target orbital energies are necessary [15].

III. EXPERIMENTAL DETAILS

The experiments involved the low- and high-energy ion beams from two different accelerator facilities. In the first part, a newly installed electron cyclotron resonance (ECR) ion-source based accelerator (ECRIA) at Tata Institute of Fundamental Research (TIFR), Mumbai was used to produce low energy (∼0.5–2 a.u.) He-like C and O ions [23]. In the second part, high-energy C and O ions (velocity, $v = 7$ to 15 a.u.) were produced in the 14-MV tandem Pelletron accelerator at TIFR. In some cases other charge states of C and also O ions were also used. The ECR ion source is mounted on a high-voltage deck (300 kV).

In brief, a Wiley McLaren type of recoil-ion time-of-flight spectrometer was used. Electrons and ions are extracted in opposite directions by a static electric field of 250 V/cm applied in the interaction region in the case of high-energy ion impact. For low-energy ion impact, to avoid the projectile beam deflection, an extraction field of only 30 V/cm was applied. Ions were detected, after passing through the acceleration (∼700 V/cm) and drift regions, by the channel electron multipliers (CEMs). Collection efficiencies for ions and electrons in both field conditions were estimated by simulation using SIMION software.

A narrow slit was placed in front of the electron CEM to reduce the excessive count rate. A gaseous target of uracil was produced by heating the (99% pure, Sigma-Aldrich) powder in an oven. The molecules effused through a nozzle of diameter 1 mm. The oven temperature of 160 °C was sufficient to get enough vapor density in the interaction region. Maintaining a uniform flow of molecules throughout the experiments was a crucial and challenging task. To ensure this, the oven temperature was raised very slowly and a quartz crystal thickness monitor was suitably mounted to monitor the flow of molecules throughout the experiments. The variation of the deposition rate, if at all, was very smooth and was found to vary by about 5–10 % over a long period, i.e., about 10 h. The absolute error (20–25 %) includes this variation. The chamber pressure was better than 4×10^{-7} Torr. The well-collimated ion beams were crossed with a gaseous uracil target in the source region between the pusher and puller plates. The electron and ion CEM signals were used as start and stop signals, respectively, in a single-hit time-to-amplitude converter. A CAMAC based data acquisition system was used.

IV. RESULTS

Figure 1 displays a typical time-of-flight (TOF) spectrum of uracil breakup in collisions with 42 MeV bare C-ions. Similar spectra were also observed in case of all other projectiles energies and charge states. The ions of $m/q = 112$ ($C_4H_4N_2O_2^+$, i.e., Ur^+), 69 ($C_3H_3NO^+$), 42 ($C_2H_2O^+$), 28 ($HCNH^+$), and 1 (H^+) are shown. The mass fragment 69 is formed by the loss of HCNO (mass 43) from the parent cation by a Retro-Diels-Alder reaction and involves the rupture of two bonds in the parent cation. Further fragmentation of $C_3H_3NO^+$ leads to the lower mass ions. Possible and energetically favorable structures of the fragments have been reported by Jochims *et al.* [24]. The strongest peak is observed at $m/q = 42$. Similar fragments have been observed in photon-, ion-, and electron-impact ionization of uracil [24–29]. The fragmentation distributions have been investigated for all the energies and were found to match with the 70 eV electron-impact data [30]. Double ionization of uracil was not observed. The yield of mass fragment 28 ($HCNH^+$) was obtained by background (N_2) subtraction, which was 70% of the total yield of $m/q = 28$.

The data from two experiments (low energy and high energy) were normalized for deposition rate and collection efficiencies. In fact, the experiments were repeated several times in order to check consistency. The TOF spectra were recorded for the He-like C and O ions with energy ranging

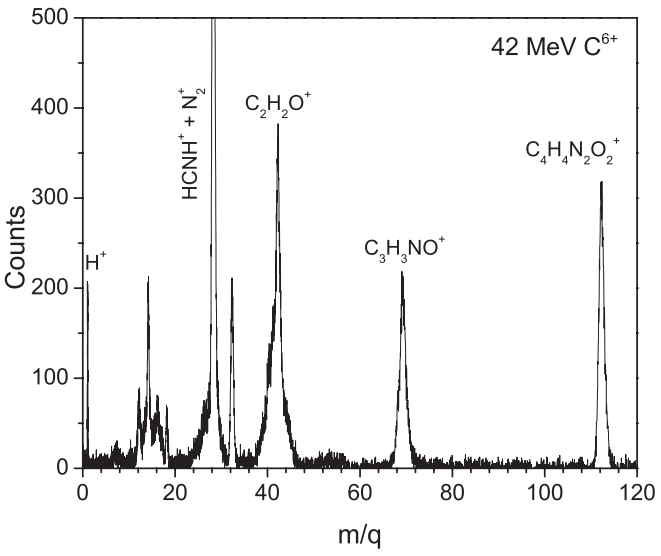

FIG. 1. Typical TOF spectrum of uracil.

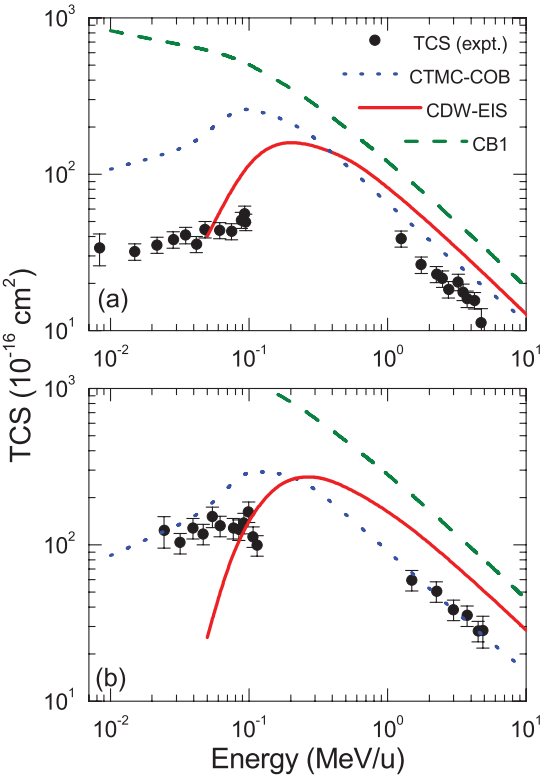

FIG. 2. (Color online) Absolute TCS (fragmentation plus ionization) of uracil in collisions with (a) C^{4+} and (b) O^{6+}.

from 100 keV to 1.6 MeV (ECR ion source) and from 15 to 78 MeV (Pelletron). The addition of areas under all (parent plus fragment) the ion peaks gives the total ionization yield. This was then converted to the absolute total ionization cross section (TCS) by adopting a different normalization procedure, based on continuum and Auger electron spectroscopy of uracil in an independent collision experiment. We have measured the electron double differential cross section (DDCS) spectrum using an electrostatic hemispherical analyzer [31]. Bare carbon ions with an energy of 42 MeV were used (for which TCS measurements have been carried out). The KLL Auger lines of C, N, and O were detected for the uracil target. The absolute KLL Auger cross section for the O_2 molecule was determined separately using a static gas condition, which was then used to normalize the electron DDCS data of uracil. Further, from the integration of the measured angular distributions the total electron emission cross section for uracil was determined, which was then used to normalize the TCS data shown in Fig. 2. Figure 2(a) shows the absolute TCS of all recoil ions (i.e., fragmentation peaks plus Ur^+) of uracil in collisions with (0.1–57)-MeV C^{4+} projectile ions. This definition of TCS, which implicitly includes the transfer ionization and excludes the capture process, can be termed the total electron emission cross section. At low energies the cross section increases as the impact energy is increased and then saturates. The cross sections fall sharply with energy in the high-energy region. This is expected since the ionization cross sections peak in the intermediate-energy range and fall in the low- as well as the high-energy range. The CTMC-COB, CB1, and CDW-EIS calculations are also shown. A comparison shows good qualitative agreement between the experimental data for C^{4+} and the theory in the high-energy range but indicates deviations in the low-energy range, which is not unexpected for quantum-mechanical models due to their perturbative nature. In the low-energy collisions the Auger electron emission following multiple-electron capture can also contribute to the spectrum studied, which is not included in the models here. The CTMC-COB calculation is higher compared to the high-energy data only by a factor of 1.5. For the CDW-EIS calculation this factor is about 2. In the low-energy region, the CDW-EIS calculation gives a sharp fall and crosses the data at 0.06 MeV/u, whereas the CTMC-COB calculation, although overestimating the data, gives a better energy dependence. In the case of the O^{6+} projectile [Fig. 2(b)], the agreement with the CTMC-COB calculation at the higher-energy part is excellent. The CTMC-COB calculation also gives better agreement below 0.05 MeV/u. The better agreement with the model in the case of the O projectile compared to that for C ions is only incidental. The CB1 calculations do not show the observed fall of cross sections in the low-energy ion impact. To describe the low-energy region it should be interesting to apply the quantum-mechanical approach based on the basis generator method recently developed by Lüdde *et al.* [32] in the context of a water molecule. The absolute error bars are shown on the first and last points of the TCS spectra. Relative error bars (∼12%) are shown on the rest of the data points. Given the complication of the collision system, the quantitative and qualitative agreements with the models are encouraging. However, it should be mentioned that since the present data i.e., TCSs (fragmentation as well as ionization), are obtained in coincidence with electrons emitted, they do not include the contributions from electron capture events, but do include the transfer-ionization (TI) process. The theoretical models do not include electron capture and the TI events. In the experimental data the contribution of the TI events is expected to be very small in the high-velocity regime. The contribution of the TI events in the low-velocity regime can be somewhat larger, which cannot be separated in the experiment. This may explain the better qualitative agreement (i.e., the slope) in the higher-energy range in comparison to the low-energy range. In the lower-energy range there is a scope of further work regarding the theoretical model as well as experiments that include coincidence with postcollision projectile charge states.

The ionization and fragmentation processes and thereby the energy loss of the projectiles depend on the perturbation strength ($P = \frac{q}{v}$) of the collision, which depends only on the q of the ions for a fixed velocity. The CTMC-COB (dotted line), CDW-EIS (solid line), and CB1 (dashed line) calculations show good qualitative agreement with experimental data [Figs. 3(a) and 3(b)]. The figure displays scaled theoretical numbers for a comparison with the experimental data. To study the effect of nuclear charge Z on the TCSs, C and O ions with the same velocity were used. We observe that the TCSs were the same for the same charge states of C and O ions and thus appear to be independent of Z. One normally finds a quadratic q dependence of the single ionization of atoms in fast collisions, which is well known from experiments and well predicted by first-order perturbative approach. However, in the case of such large molecules it is not obvious whether such a

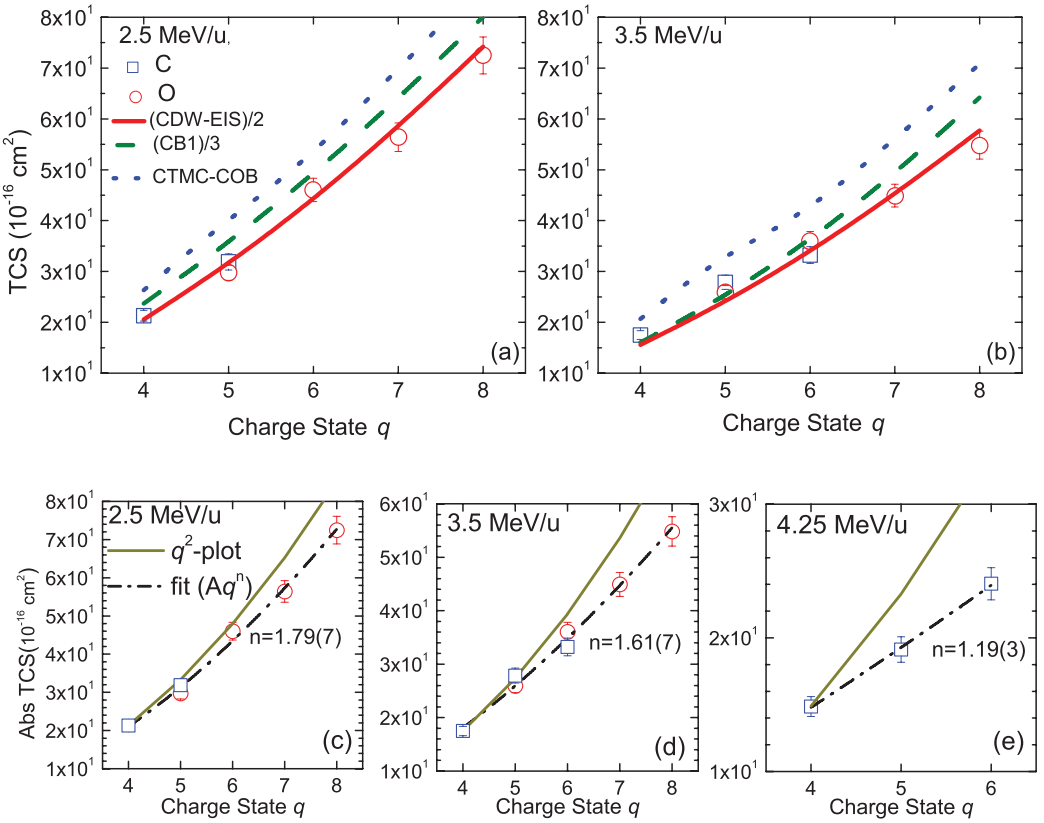

FIG. 3. (Color online) [(a) and (b)] The q dependence of the total ionization cross sections along with the model calculations. [(c), (d) and (e)] show the fitted TCS (dashed-dotted line) along with the q^2 plot (solid lines).

q^2 dependence can be used in modeling even for fast collisions and therefore the TOF spectra for were investigated for C and O ions with different q. The q dependence of the TCSs at different energies was fitted to a TCS equal to Aq^n. The n is found to be 1.79(7) and 1.61(7) at these two energies [see Figs. 3(c) and 3(d)]. A similar study at 4.25-MeV/u C ions gives the value of n as low as 1.19(3) [Fig. 3(e)]. The deviation of the data from the expected q^2 dependence (shown by dotted lines) is obvious from the plots. At all other energies similar values of n (i.e., between 1.8 and 1.2) were obtained. These studies will be extended to higher values of q in order to investigate this behavior over a wider range projectile charge state. Therefore, at this energy range, the TCS seems to deviate from the q^2 dependence, as one expects in an ion-atom collision system. It should be mentioned that this behavior is also different from other many-body systems, such as fullerenes [33,34], for which a linear q dependence was observed. In this sense the n value for uracil falls between simple atoms and fullerene.

V. CONCLUSION

The absolute TCSs were measured for highly charged C and O ion impact on an RNA base molecule, uracil, over a wide energy range, broadly included in the Bragg peak region, i.e., between 100 keV and 78 MeV. A technique for absolute normalization based on the continuum and KLL Auger electron spectroscopy has been developed. The calculations for uracil were developed using the CDW-EIS and CB1 approximations to compare with the present data. The CDW-EIS and CTMC-COB calculations, in general, were in good qualitative agreement with the energy dependence, except for low energy. The slope of the energy distribution is well reproduced by the quantum-mechanical models at high energies. The classical CTMC-COB model provides excellent agreement with the data at higher energies. The TCS is shown to deviate from the quadratic q dependence, which is well known in the case of ion-atom collisions. The observed q dependence and the Z independence of the TCSs are in agreement with the models used. The results may be of importance in providing the input required for model calculations for radiation damage as well as for a qualitative understanding of molecular collision physics involving large molecules, in general, and for DNA and RNA base molecules, in particular.

ACKNOWLEDGMENTS

The authors acknowledge the Pelletron accelerator team for smooth running of the machine. We also thank C. A. Desai, W. Fernandes, K. V. Thulasiram, and N. Mhatre for their help during the ECR-based experiments and D. Misra for fruitful discussions.

[1] J. deVries, R. Hoekstra, R. Morgenstern, and T. Schlatholter, Phys. Rev. Lett. **91**, 053401 (2003).
[2] R. Brédy, J. Bernard, L. Chen, M. C. Buchet-Poulizac, and S. Martin, Nucl. Instrum. Methods Phys. Res. B **261**, 114 (2007).
[3] M. Imhoff, Z. Deng, and M. A. Huels, Int. J. Mass Spectrom. **245**, 68 (2005).
[4] J. Bernard, R. Brédy, L. Chen, S. Martin, and B. Wei, Nucl. Instr. Meth. Phys. Res. B **245**, 103 (2006).
[5] T. Schlathölter, F. Alvarado, S. Bari, A. Lecointre, R. Hoekstra, V. Bernigaud, B. Manil, J. Rangama, and B. Huber, Chem. Phys. Chem. **7**, 2339 (2006).
[6] F. Alvarado, S. Bari, R. Hoekstra, and T. Schlatholter, Phys. Chem. Chem. Phys. **8**, 1922 (2006).
[7] B. Coupier, B. Farizon, M. Farizon, M. J. Gaillard, F. Gobet, N. V. de Castro Faria, G. Jalbert, S. Ouaskit, M. Carré, B. Gstir, G. Hanel, S. Denifl, L. Feketeova, P. Scheier, and T.D. Märk, Eur. Phys. J. D **20**, 459 (2002).
[8] P. Moretto-Capelle and A. Le Padellec, Phys. Rev. A **74**, 062705 (2006).
[9] J. Tabet, S. Eden, S. Feil, H. Abdoul-Carime, B. Farizon, M. Farizon, S. Ouaskit, and T. D. Mark, Phys. Rev. A **82**, 022703 (2010).
[10] Y. Iriki, Y. Kikuchi, M. Imai, and A. Itoh, Phys. Rev. A **84**, 032704 (2011).
[11] H. Deutsch, K. Becker, S. Matt, and T. D. Märk, Int. J. Mass Spectrom. **197**, 37 (2000).
[12] Y. K. Kim and M. E. Rudd, Phys. Rev. A **50**, 3954 (1994).
[13] M. C. Bacchus-Montabonel, M. Labuda, Y. S. Tergiman, and J. E. Sienkiewicz, Phys. Rev. A **72**, 052706 (2005).
[14] I. Abbas, C. Champion, B. Zarour, B. Lasri, and J. Hanssen, Phys. Med. Biol. **53**, N41 (2008).
[15] H. Lekadir, I. Abbas, C. Champion, O. Fojon, R. D. Rivarola, and J. Hanssen, Phys. Rev. A **79**, 062710 (2009).
[16] C. Dal Cappello, P. A. Hervieux, I. Charpentier, and F. Ruiz-Lopez, Phys. Rev. A **78**, 042702 (2008).
[17] C. Champion, H. Lekadir, M. E. Galassi, O. Fojón, R. D. Rivarola, and J. Hanssen, Phys. Med. Biol. **55**, 6053 (2010).
[18] O. V. Shishkin, L. Gorb, A. V. Luzanov, M. Elstner, S. Suhai, and J. Leszczynski, J. Mol. Struct. (Theochem) **625**, 295 (2003).
[19] M. J. Frisch, G. W. Trucks, H. B. Schlegel *et al*., GAUSSIAN09, Revision A.02 (Gaussian, Inc., Wallingford, CT, 2009).
[20] Dž. Belkic, R. Gayet, and A. Salin, Phys. Rep. **56**, 279 (1979).
[21] P. D. Fainstein, V. H. Ponce, and R. D. Rivarola, J. Phys. B **21**, 287 (1988).
[22] M. E. Galassi, R. D. Rivarola, and P. D. Fainstein, Phys. Rev. A **70**, 032721 (2004).
[23] A. N. Agnihotri, A. H. Kelkar, S. Kasthurirangan, K. V. Thulasiram, C. A. Desai, W. A. Fernandez, and L. C. Tribedi, Phys. Scr. **T144**, 014038 (2011).
[24] H.-W. Jochims, M. Schwell, H. Baumgartel, and S. Leach, Chem. Phys. **314**, 263 (2005).
[25] T. Schlathölter, R. Hoekstra, and R. Morgenstern, Int. J. Mass Spectrom. **233**, 173 (2004).
[26] S. Denifl, B. Sonnweber, G. Hanel, P. Scheier, and T.D. Märk, Int. J. Mass Spectrom. **238**, 47 (2004).
[27] M. Imhoff, Z. Deng, and M. A. Huels, Int. J. Mass Spectrom. **262**, 154 (2007).
[28] NIST Chemistry web book [http://webbook.nist.gov/cgi/cbook.cgi?ID=C66228&Units=SI&Mask=200].
[29] S. Feil, K. Gluch, S. Matt-Leubner, P. Scheier, J. Limtrakul, M. Probst, H. Deutsch, K. Becker, A. Stamatovic, and T. D. Märk, J. Phys. B **37**, 3013 (2004).
[30] J. M. Rice, G. O. Dudek, and M. Barber, J. Am. Chem. Soc. **87**, 4569 (1965).
[31] D. Misra, K. V. Thulasiram, W. Fernandes, A. H. Kelkar, U. Kadhane, Ajay Kumar, Yeshpal Singh, L. Gulyás, and Lokesh C. Tribedi, Nucl. Instr. Meth. Phys. Res. B **267**, 157 (2009).
[32] H. J. Ludde, T. Spranger, M. Horbatsch, and T. Kirchner, Phys. Rev. A **80**, 060702(R) (2009).
[33] A. H. Kelkar, U. Kadhane, D. Misra, L. Gulyas, and L. C. Tribedi, Phys. Rev. A **82**, 043201 (2010).
[34] U. Kadhane, A. Kelkar, D. Misra, A. Kumar, and L. C. Tribedi, Phys. Rev. A **75**, 041201(R) (2007).